

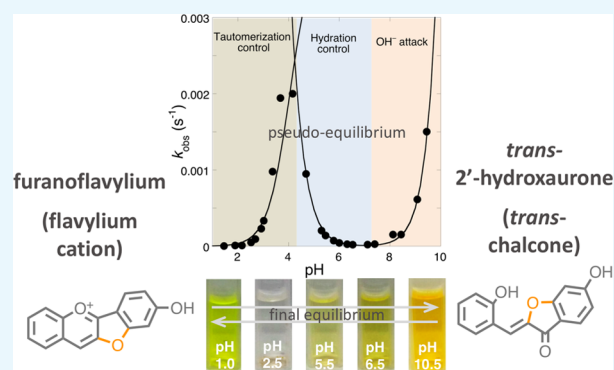
pH-Dependent Multistate System Generated by a Synthetic Furanoflavylium Compound: An Ancestor of the Anthocyanin Multistate of Chemical Species

A. Alejo-Armijo,^{1b} A. Jorge Parola,^{*,1b} and Fernando Pina^{*,1b}

LAQV-REQUIMTE, Departamento de Química, Faculdade de Ciências e Tecnologia, Universidade NOVA de Lisboa, 2829-516 Caparica, Portugal

S Supporting Information

ABSTRACT: The multistate of chemical species generated by 4'-hydroxy-3,2'-furanoflavylium is similar to that of anthocyanins and related compounds. This furanoflavylium multistate system was fully characterized by UV–visible and NMR spectroscopy, allowing determination of the respective equilibrium and rate constants. In contrast to the multistate generated by flavylium cations derived from anthocyanins and related compounds, the furanoflavylium multistate is characterized by much slower hydration and tautomerization (pyran ring opening–closing). In addition, the *cis*–*trans* isomerization of the chalcones of this system (2'-hydroxyaurones) is extremely slow when compared with anthocyanins. The observed similar order of magnitude for tautomerization and isomerization rate constants leads to peculiar kinetics from the flavylium cation (pH = 1) to the stable *trans*-chalcone (higher pH values). The hemiketal appears and disappears during the first stages of the kinetics, which gives the intermediate *cis*-chalcone (pseudo-equilibrium). This last species disappears in a much slower process, as fully characterized by ¹H NMR, to give the final *trans*-chalcone.



INTRODUCTION

In the past years, it was reported that a network of chemical species originating in solution from anthocyanins, that is, its multistate of chemical species, can be found in structurally related compounds. Anthocyanidins,^{1,2} deoxyanthocyanidins,^{3–5} styrylflavylium,⁶ naphthoflavylium,⁷ and other synthetic flavylium compounds⁸ are examples of molecules that generate the same multistate observed in anthocyanins. In some cases, other chemical species not appearing in the anthocyanin multistate are formed, such as flavanones from 2'-hydroxyflavylium compounds⁹ and 2,2'-spirobis[chromene] derivatives from 2,6-bis(arylidene)cyclohexanones.^{10,11,a}

Aurones are a class of flavonoids that are responsible for giving color to mosses, ferns, and marine brown algae, as well as bright yellow colors to some flowers.¹² The subclass of 2'-hydroxyaurones is able to form furanoflavylium cations, such as riccionidin A.¹³ In this work, we report a model compound, furanoflavylium **1**, and the multistate of species originating from it in aqueous solution, in particular, its corresponding 2'-hydroxyaurone, **2** (see Scheme 1). To our knowledge, the term furanoflavylium was coined by Seshadri^{14,b} to designate flavylium compounds containing a furan ring between rings C and B, with the oxygen linking positions 3 and 2', like in riccionidin A.

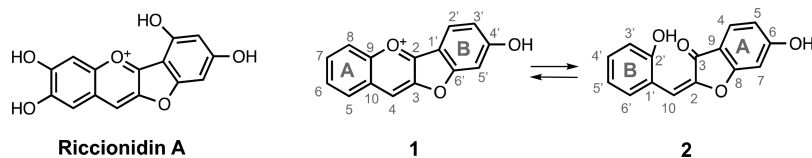
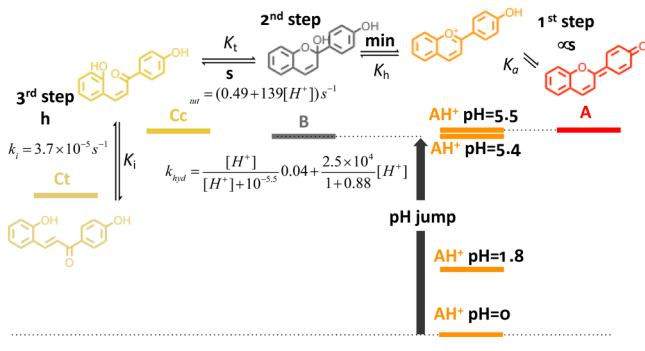
Anthocyanin history demonstrated that synthetic flavylium compounds are very important to fully understand anthocyanin multistate kinetics and thermodynamics; in particular, the inclusion of *trans*-chalcone in the anthocyanin multistate should be considered.⁸ In this work, we synthesized and fully characterized the multistate of chemical species originating from the compound 4'-hydroxy-3,2'-furanoflavylium (8-hydroxybenzofuro[3,2-*b*]chromen-5-ium, **1**) hydrogen sulfate. Similar to the role played by synthetic flavylium compounds on the comprehension of the anthocyanin multistate, our present results could pave the way for future descriptions of the multistates of naturally occurring furanoanthocyanins.^{15,c} For this reason we chose as a model compound a very simple furanoflavylium (**1**), where we introduced only one hydroxyl group (to allow formation of the quinoidal base species; see below). The main scope of this work is to investigate the multistate of species of furanoflavylium cations, which includes 2'-hydroxyaurones (see below, Scheme 3), and compare it with the known multistate of flavylium salts that includes 2-hydroxychalcones (also designated as retrochalcones; see Scheme 2).

Received: December 31, 2018

Accepted: February 5, 2019

Published: February 22, 2019

Scheme 1. Riccionidin A, 4'-Hydroxy-3,2'-furanoflavylum (1), and Its Respective 2'-Hydroxyaurone (2)

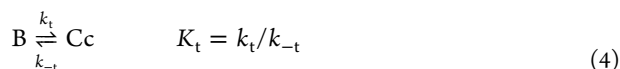
Scheme 2. Three Distinct Kinetic Steps Occurring in Anthocyanins and Related Compounds after a Direct pH Jump Illustrated Here for 4'-Hydroxyflavylum (the Flavylum Analogue of Furanoflavylum 1)^{19,20}

State of the Art in Anthocyanin Multistate. Anthocyanins and other flavylum salt derivatives are characterized by the existence of three kinetic steps that are well separated with time, allowing the study of each one separately. The energy level diagram presented in Scheme 2 for 4'-hydroxyflavylum is appropriate to account for the chemistry of the network of chemical species present in flavylum salts multistates.^{16–18}

At lower pH values, the flavylum cation (AH^+) is the stable species. Raising the pH (defined as direct pH jumps) leads to the formation of a quinoidal base (A) upon proton transfer to water (eq 1). This reaction is by far the fastest of the multistate. The rate of this process, k_{1d} (eq 2), is very fast (μs) and requires special techniques, such as temperature jumps,²¹ to be adequately characterized. However, representation of the pH-dependent absorption spectra taken 10 ms after the direct pH jump by means of stopped-flow experiments permits calculation of the value of K_a . During the subsequent kinetic processes, AH^+ and A remain in equilibrium with a ratio $[\text{A}]/[\text{AH}^+] = K_a/[\text{H}^+]$.



The next step, second step in Scheme 2, is controlled by the hydration reaction. Unless for very acidic solutions, which are not accessible by direct pH jumps, the hydration reaction in eq 3 (seconds to minutes) is slower than tautomerization in eq 4 (milliseconds to seconds).

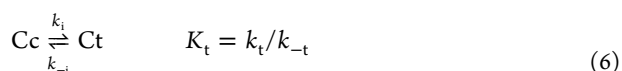


The rate constant of this step is given by eq 5

$$\begin{aligned} k_{2d} &= X_B k_h + X_{Cc} k_{-h} [\text{H}^+] \\ &= \frac{[\text{H}^+]}{[\text{H}^+] + K_a} k_h + \frac{1}{1 + K_t} k_{-h} [\text{H}^+] \end{aligned} \quad (5)$$

where X_B and X_{Cc} are the mole fractions of B and Cc, respectively, in eq 4.

Finally, the system reaches its thermodynamic equilibrium upon *cis*–*trans* isomerization of the chalcone species, a process that takes hours or days (eq 6).



Considering that the isomerization is much slower than the other processes, all species except Ct can be considered in equilibrium during the isomerization. The transient state that is reached when AH^+ , A, B, and Cc are in equilibrium, before formation of significant amounts of Ct, is defined as “pseudo-equilibrium”.

The rate constant of the isomerization step is given by eq 7

$$k_{3d} = X_{Cc} k_i + k_{-i} = \frac{K_h K_t k_i}{[\text{H}^+] + K_a} + k_{-i} \quad (7)$$

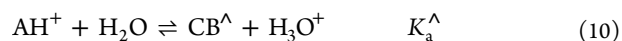
where X_{Cc} is the mole fraction of *cis*-chalcone at the pseudo-equilibrium and K_a^\wedge is the constant of the pseudo-equilibrium (see eqs 10 and 11 below).

The overall equilibrium, in spite of its complexity, can be described by a simple acid–base equilibrium involving the flavylum cation and its conjugate base, CB, composed of the other species: $[\text{CB}] = [\text{A}] + [\text{B}] + [\text{Cc}] + [\text{Ct}]$.²²



$$K'_a = K_a + K_h + K_h K_t + K_h K_t K_i \quad (9)$$

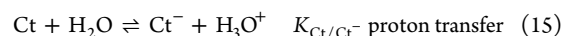
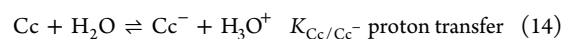
The pseudo-equilibrium (eq 10) is defined by a similar equation where Ct is now excluded: $[\text{CB}^\wedge] = [\text{A}] + [\text{B}] + [\text{Cc}]$.



$$K_a^\wedge = K_a + K_h + K_h K_t \quad (11)$$

It is possible to extend the study of the kinetics and thermodynamics of the equilibrium and pseudo-equilibrium to the basic region, by considering consecutive deprotonations of the species (eqs 12–15 and 16–19).

Second set of acid–base equilibria



Third set of acid–base equilibria

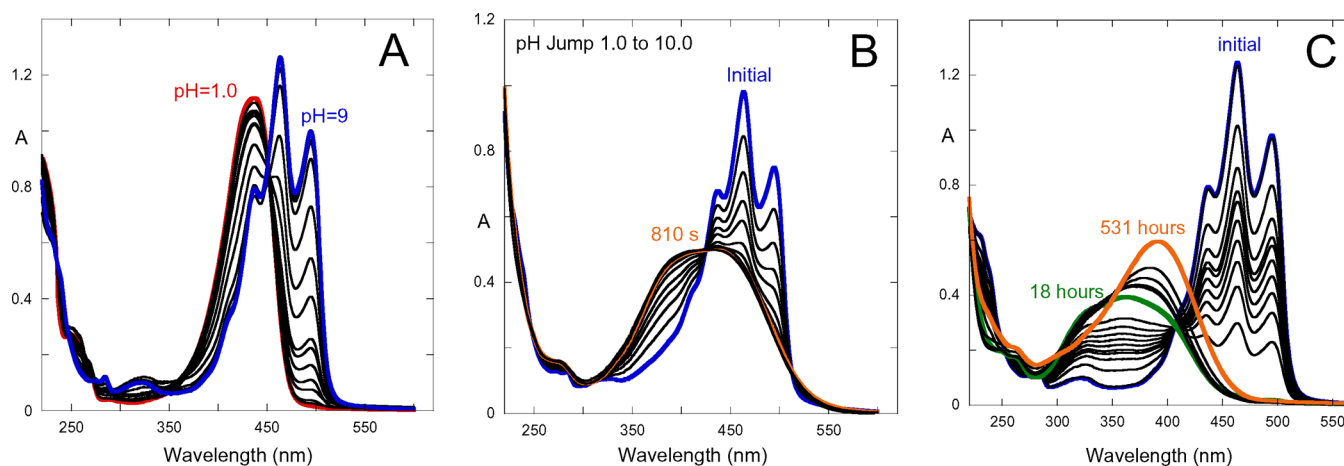


Figure 1. (A) Spectral variations of compound **1** (2.31×10^{-5} M), taken 1 min after a direct pH jumps to $1.0 < \text{pH} < 9.0$. The spectral variations are accounted for by an acid–base equilibrium between AH^+ and A , with $\text{p}K_a = 3.6$ (eq 1). (B) Spectral variations after a direct pH jump to 10.0. (C) Spectral variations after a direct pH jump from $\text{pH} = 1.0$ to 5.5.

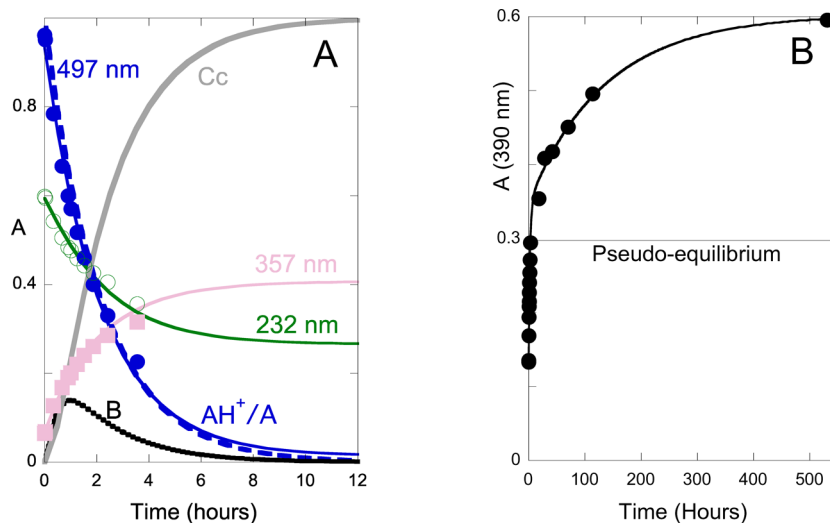
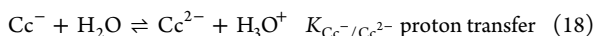
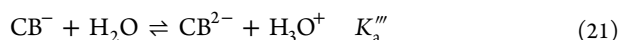
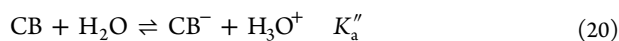


Figure 2. (A) Absorbance as a function of time after a direct pH jump of compound **1** to $\text{pH} = 5.5$ toward the pseudo-equilibrium. The kinetic traces can be fitted by two consecutive reactions with rate constants of 1.3×10^{-4} and $6.0 \times 10^{-4} \text{ s}^{-1}$. (B) A second and much slower step that transforms the green spectrum of Figure 1c into the orange one can be fitted with a rate constant of $2.8 \times 10^{-6} \text{ s}^{-1}$.



This system is thus equivalent to a single polyprotic acid, with eq 8 accounting for the first global acid–base equilibrium, K_a' , and eqs 20 and 21 accounting for the second and third acid–base equilibria, respectively, K_a'' and K_a''' ,



where

$$[\text{CB}^-] = [\text{A}^-] + [\text{B}^-] + [\text{Cc}^-] + [\text{Ct}^-] \quad (22)$$

$$[\text{CB}^{2-}] = [\text{A}^{2-}] + [\text{B}^{2-}] + [\text{Cc}^{2-}] + [\text{Ct}^{2-}] \quad (23)$$

The relations between the global acid–base constants, K_a'' and K_a''' , and the equilibrium constants for each reaction are given, respectively, by eqs 24 and 25.

$$K_a'' = (K_{\text{A}^-/\text{A}^{2-}}K_a + K_{\text{B}^-/\text{B}^{2-}}K_h + K_{\text{Cc}^-/\text{Cc}^{2-}}K_hK_t + K_{\text{Ct}^-/\text{Ct}^{2-}}K_hK_tK_i)/K_a' \quad (24)$$

$$K_a''' = (K_{\text{A}^-/\text{A}^{2-}}K_{\text{A}^-/\text{A}^{2-}}K_a + K_{\text{B}^-/\text{B}^{2-}}K_{\text{B}^-/\text{B}^{2-}}K_h + K_{\text{Cc}^-/\text{Cc}^{2-}}K_{\text{Cc}^-/\text{Cc}^{2-}}K_hK_t + K_{\text{Ct}^-/\text{Ct}^{2-}}K_{\text{Ct}^-/\text{Ct}^{2-}}K_hK_tK_i)/K_a'K_a'' \quad (25)$$

These expressions can be generalized to further deprotonated species, but in general, anthocyanins are not stable in basic medium.

In conclusion, in spite of the complexity of this system, the flavylium cation can be considered a simple polyprotic acid, and the respective acidity constants are straightforwardly calculated from the inflection points of the representation of the absorbance versus pH.

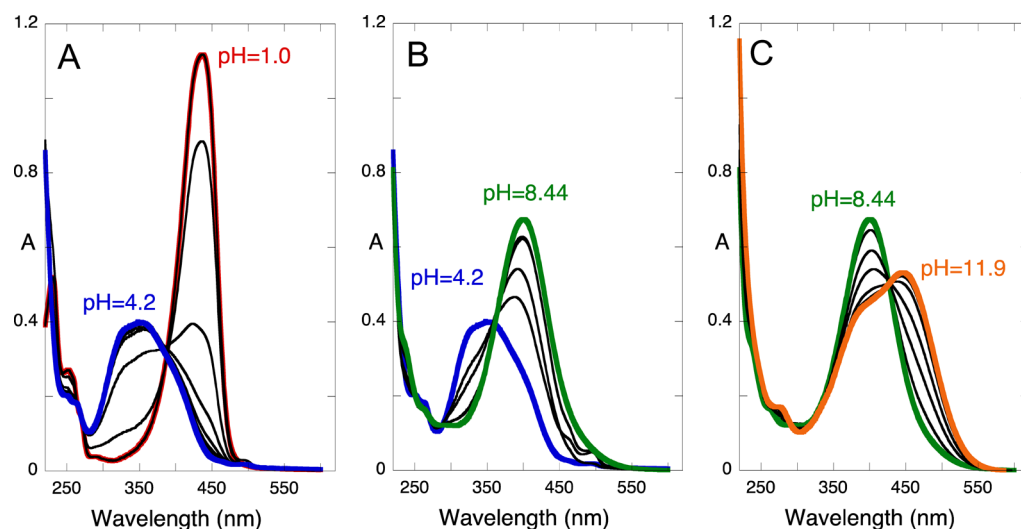


Figure 3. Spectral variations of compound **1** (2.31×10^{-5} M) approximately 20 h after direct pH jumps to pH values in the ranges: (A) $1.0 \leq \text{pH} \leq 4.2$, (B) $4.2 \leq \text{pH} \leq 8.44$, and (C) $8.44 \leq \text{pH} \leq 11.9$. The data could be fitted with $\text{p}K_a^{\wedge} = 1.8$, $\text{p}K_a^{\wedge\wedge} = 6.55$, and $\text{p}K_a^{\wedge\wedge\wedge} = 9.2$ for the three pH ranges.

RESULTS AND DISCUSSION

Furanoflavylium **1** was synthesized as its hydrogen sulfate salt from the condensation of salicylaldehyde with 6-hydroxybenzofuran-3(2*H*)-one in a mixture of acetic acid and sulfuric acid. To our knowledge, the only synthesis of furanoflavylium salts reported so far is that of Seshadri, where compound **1** as its chloride salt was also reported.¹⁴

Similarly to some synthetic flavylium compounds that have been used as models for anthocyanins such as 4'-hydroxyflavylium, the kinetics of compound **1** taking place after direct pH jumps from a very acidic solution to acidic/moderately basic media or to very basic media behave differently.²³ The reason is that in acidic/moderately basic medium, the quinoidal base does not hydrate, a breakthrough discovered by Brouillard and Dubois.²⁴ However, in very basic solutions, the hydroxide anion attacks the quinoidal base to give ionized *cis*-chalcone, and the respective rate is directly proportional to the hydroxide concentration.²⁵ This behavior is illustrated in Figure 1a,b for compound **1**. The spectral variations taken 1 min after a direct pH jump to the range $1.0 < \text{pH} < 9$ (Figure 1a) show an equilibrium between the flavylium cation, AH^+ , and the quinoidal base, A. The spectra are compatible with an acid–base equilibrium between AH^+ and A with $\text{p}K_a = 3.6$, according to eq 1 and the first step in Scheme 2. Upon a pH jump to $\text{pH} = 10$ (Figure 1b), after 810 s, the quinoidal base is already consumed to give an absorption spectrum that was assigned to ionized Cc (see below).

The spectral variations after a direct pH jump to $\text{pH} = 5.5$ are shown in Figure 1c. The kinetics takes place in two different time scales: (i) after approximately 18 h, the absorption spectrum is that of chalcone (green line), and (ii) after 531 h, another red-shifted chalcone-type absorption spectrum is formed (orange line). The NMR data reported below allows us to conclude that the green spectrum can be attributed to *cis*-chalcone and the orange one to *trans*-chalcone. Moreover, the NMR data also shows that during the first hours, the hemiketal, B, grows in amount and then decreases before reaching the pseudo-equilibrium. This particular aspect needs a further explanation because it is not observed in anthocyanins.

To get more insight into the kinetics toward the pseudo-equilibrium and further to the equilibrium, a series of direct pH

jumps were performed, as exemplified for $\text{pH} = 5.5$ in Figures 1c (spectra) and 2 (kinetic traces and fittings). Regarding the kinetics toward the pseudo-equilibrium and taking into account that the hemiketal, B, is formed and decreases during the first stages of the process, a kinetic model of the type $\text{AH}^+/\text{A} \rightarrow \text{B} \rightarrow \text{Cc}$ was considered.^d

In anthocyanins and related compounds, the tautomerization is much faster than hydration, unless for very acidic pH values not accessed by direct pH jumps. In other words, as soon as B is formed, it equilibrates with Cc to give the pseudo-equilibrium in a ratio that is given by $K_t = [\text{Cc}]/[\text{B}]$, as seen in the second step in Scheme 2. In the case of compound **1**, the system was treated considering two consecutive reactions (Figure 2a). In spite of the high estimated error (ca. 20%), a fitting with global rate constants equal to 1.3×10^{-4} and $6.0 \times 10^{-4} \text{ s}^{-1}$ was achieved (Figure 2a). The pseudo-equilibrium is reached through the hydration reaction, exhibiting the slower constant, followed by the slightly faster tautomerization reaction. The fact that the tautomerization is only approximately 5-fold faster than hydration is the reason why at the initial stages of the kinetic process, there is some appearance and further disappearance of B. A further slower process with a rate constant equal to $2.8 \times 10^{-6} \text{ s}^{-1}$ was attributed to the formation of *trans*-chalcone, given by eq 6 and as seen in the third step in Scheme 2, as confirmed by NMR (see Figure 8 below).

A series of pH jumps like those reported in Figure 1 were carried out, and the respective absorption spectra after 20 h (at the pseudo-equilibrium) are represented in Figure 3. The pseudo-equilibrium in the pH range $1 < \text{pH} < 4.2$ with $\text{p}K_a^{\wedge} = 1.8$ is achieved between the flavylium cation and the neutral *cis*-chalcone (Figure 3a). The spectral variations reported in Figure 3b,c are compatible with the monoionized and diionized *cis*-chalcone molecules with $\text{p}K_a^{\wedge\wedge} = 6.55$ and $\text{p}K_a^{\wedge\wedge\wedge} = 9.2$.

Accurate quantitative determination of the apparent $\text{p}K_a$ values at the equilibrium (after 546 h) is not possible due to some observed precipitation in water. The following values are only rough estimations: $\text{p}K_a' \approx 1.2$, $\text{p}K_a'' \approx 5.3$, and $\text{p}K_a''' \approx 9.1$.

More information on the multistate was achieved by means of a series of reverse pH jumps carried out by the addition of acid (back to $\text{pH} = 1$) to equilibrated solutions at higher pH values. These experiments have shown that *cis*-chalcone is extremely

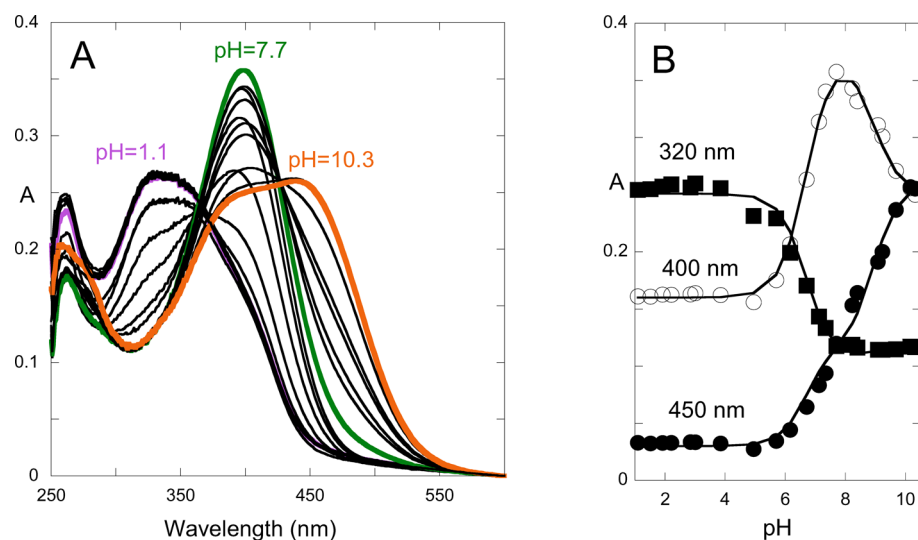


Figure 4. (A) Absorption spectra taken immediately after a series of reverse pH jumps from pseudo-equilibrated solutions of **1** (1.15×10^{-5} M) at pH = 10.3 (for 30 min) to lower pH values. (B) Traces of the absorption as a function of pH. Two inflection points of the acidity constants were obtained at pH = 6.7 and 8.9.

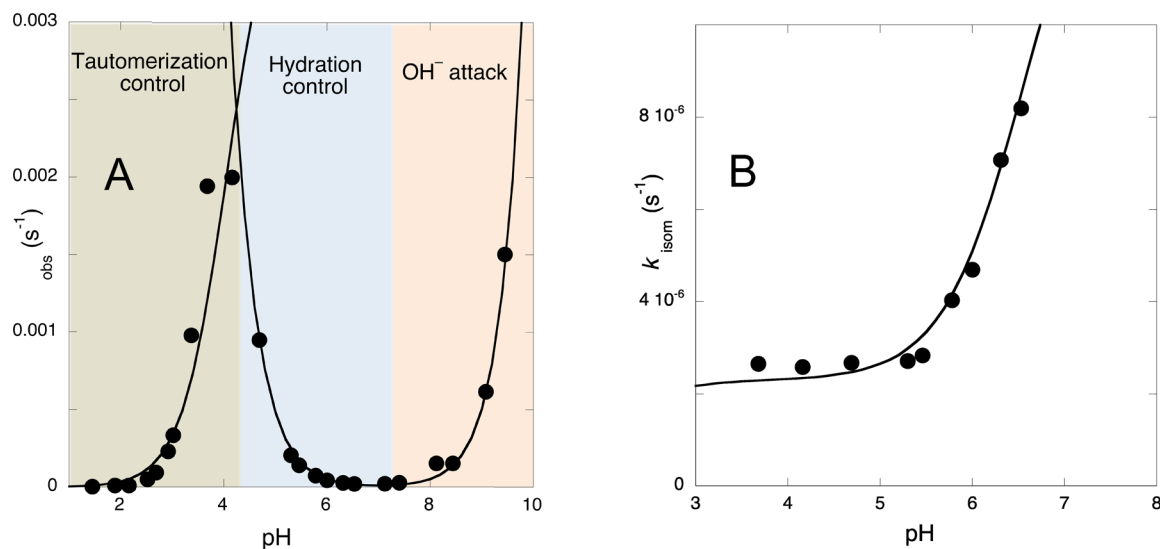


Figure 5. (A) Representation of the kinetic processes of compound **1** following a series of direct pH jumps toward the pseudo-equilibrium and (B) that from the pseudo-equilibrium to the equilibrium: $k_i = 2.3 \times 10^{-6} \text{ s}^{-1}$ (Cc to Ct) and $k_i^- = 1.5 \times 10^{-5} \text{ s}^{-1}$ (Cc⁻ to Ct⁻).

(meta)stable. For example, a reverse pH jump back to pH = 1.0 does not give back the flavylium cation in several days at room temperature. However, when the reverse pH jump is made by addition of sulfuric acid diluted in acetic acid with the solution heated at 100 °C, the characteristic absorption spectrum of the flavylium cation starts to appear.

The metastability of *trans*-chalcone in this family of compounds was previously reported for 2,3,6,8-tetrahydroxybenzofuro[3,2-*b*][1]benzopyrylium chloride (riccionidin A).²⁶ The synthesis of riccionidin A from the reaction of 2,4,5-trihydroxybenzaldehyde with 5,6-dihydroxybenzofuran-3(2*H*)-one gives *trans*-chalcone that evolves in acetic acid saturated with gaseous HCl to the respective flavylium cation in approximately 125 h at 100 °C in a percentage of 5% *trans*-chalcone and 95% flavylium cation.²⁶

Upon titration of *cis*-chalcone, the absorption spectra (Figure 4) show the presence of Cc, Cc⁻, and Cc²⁻ species, with $\text{p}K_{\text{Cc}/\text{Cc}^-} = 6.7$ and $\text{p}K_{\text{Cc}^-/\text{Cc}^{2-}} = 9.0$.

The rate constants of a series of direct pH jumps as shown in Figure 1a are represented in Figure 5. The kinetic processes regarding the evolution toward the pseudo-equilibrium (Figure 5a) have two distinct regimes. At low pH values (pH < 4), the hydration, which is proportional to $[\text{H}^+]$, should be very fast, and thus, the observed kinetics is dominated by the tautomerization process. The observed increase in this rate constant with increasing pH is related to the fraction of B available to give Cc, and the respective inflection point should reflect the $\text{p}K_{\text{h}}$. The regime in the range $4 < \text{pH} < 7$ was attributed to the hydration control as observed in anthocyanins and related compounds. The following kinetic expressions should be considered only as a semiquantitative kinetic analysis of the process.

When the hydration control is concerned, the following expression can be considered

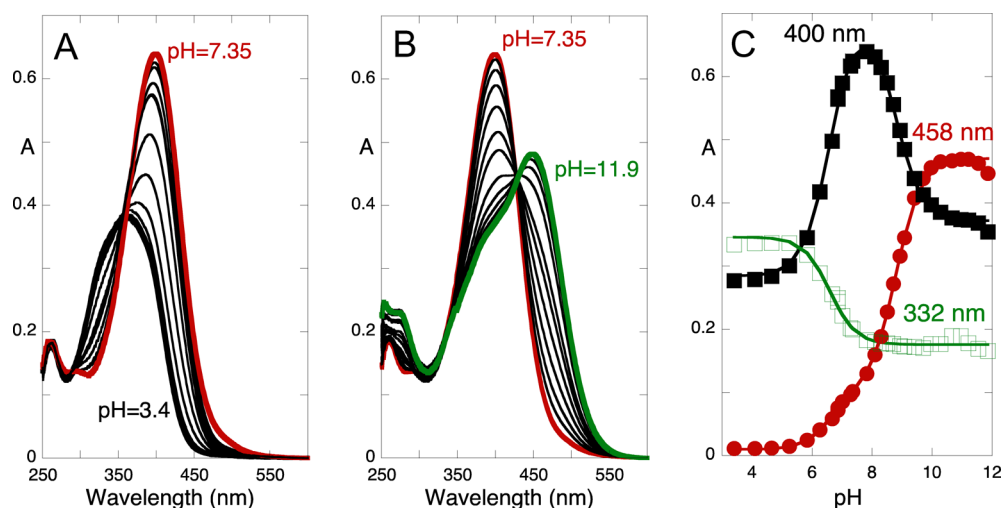


Figure 6. Absorption spectra taken immediately after a series of pH jumps (reverse or direct) from equilibrated solutions at pH = 10.3 (580 h; 2.31×10^{-5} M) to pH values in the ranges: (A) $3.4 < \text{pH} < 7.35$ and (B) $7.35 < \text{pH} < 11.9$. (C) Traces of the absorption at defined wavelengths as a function of pH; two acidity constants were obtained at pH = 6.6 and 8.8.

Scheme 3. Multistate of Chemical Reaction for 4'-Hydroxy-3,2'-furanoflavylium (1) in Acidic and Neutral Regions (under Basic Conditions, Both Chalcones Form the Monoanionic and Dianionic Species)

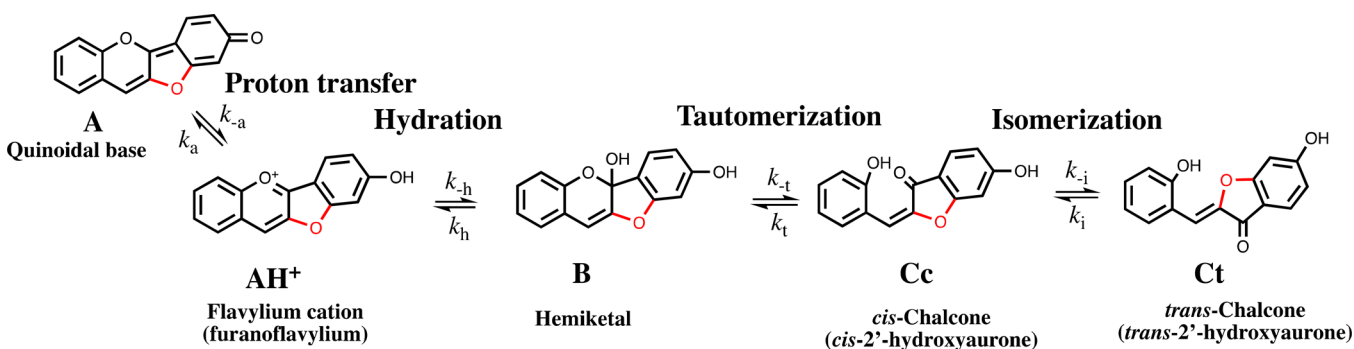


Table 1. Kinetic Parameters for Compound 1 and 4'-Hydroxyflavylium in Water

compound	$\text{p}K_a$	$\text{p}K_a'$	$\text{p}K_h$	k_h (s^{-1})	k_{-h} ($\text{M}^{-1} \text{s}^{-1}$)	k^{OH} ($\text{M}^{-1} \text{s}^{-1}$)
compound 1	3.6	1.8	4.05	0.01	$< 10^4$	50
4'-hydroxyflavylium ^{19,20}	5.5	5.0	5.4	0.09	2.5×10^4	

^aThere is not enough accuracy to measure this constant.

$$k_{\text{hyd}} = X_{\text{AH}^+}k_h + k_{-h}[\text{H}^+] = \frac{[\text{H}^+]}{[\text{H}^+] + K_a}k_h + k_{-h}[\text{H}^+] \quad (31)$$

where X_{AH^+} is the mole fraction of AH^+ in equilibrium with B. The fitting was achieved for $\text{p}K_a = 3.6$ and $k_h = 0.01 \text{ s}^{-1}$ and is independent of k_{-h} .

Regarding the tautomerization control, the species AH^+ and B are considered equilibrated because at low pH values, the hydration is much faster.

$$k_{\text{taut}} = X_B k_t + X_{\text{Cc}} k_{-t} = \frac{K_h}{[\text{H}^+] + K_h} k_t + \frac{K_t}{1 + K_t} k_{-t} \approx \frac{K_h}{[\text{H}^+] + K_h} k_t \quad (32)$$

A second approximation (by neglecting the back reaction) results from the very slow kinetics of the reverse pH jumps from Cc at the pseudo-equilibrium back to the acidic region. Fitting

was achieved for $\text{p}K_h = 4.05$ and $k_t = 0.004 \text{ s}^{-1}$. At higher pH values ($\text{pH} > 7$), the kinetics toward the pseudo-equilibrium is proportional to $[\text{OH}^-]$, and we assigned this process to hydroxide attack to the quinoidal base, as observed in synthetic flavylium compounds.²⁵ Fitting of this branch was achieved for $k^{\text{OH}} = 50 \text{ M}^{-1} \text{ s}^{-1}$.

$$k_{\text{OH}^-} = k^{\text{OH}}[\text{OH}^-] \quad (33)$$

From the pseudo-equilibrium to the equilibrium, the kinetics is very slow, Figure 5b. The following mathematical expression considers that in the pH range of Figure 5b, Cc and Cc^- are the only species at the pseudo-equilibrium and the back reaction can be neglected. Fitting was achieved for $k_i = 2.3 \times 10^{-6} \text{ s}^{-1}$ (Cc to Ct) and $k_i^- = 1.5 \times 10^{-5} \text{ s}^{-1}$ (Cc^- to Ct^-).

$$k_{\text{isom}} = X_{\text{Cc}} k_i + X_{\text{Cc}^-} k_i^- \quad (34)$$

Upon titration of *trans*-chalcone, the absorption spectra (Figure 6) show the presence of the species Ct (brown), Ct^- (red), and Ct^{2-} (green) with $\text{p}K_{\text{Ct}^-/\text{Ct}} = 6.6$ and $\text{p}K_{\text{Ct}^{2-}/\text{Ct}^-} = 8.8$.^e

Scheme 4. Energy Level Diagram of Compound 1 in Aqueous Acidic Medium

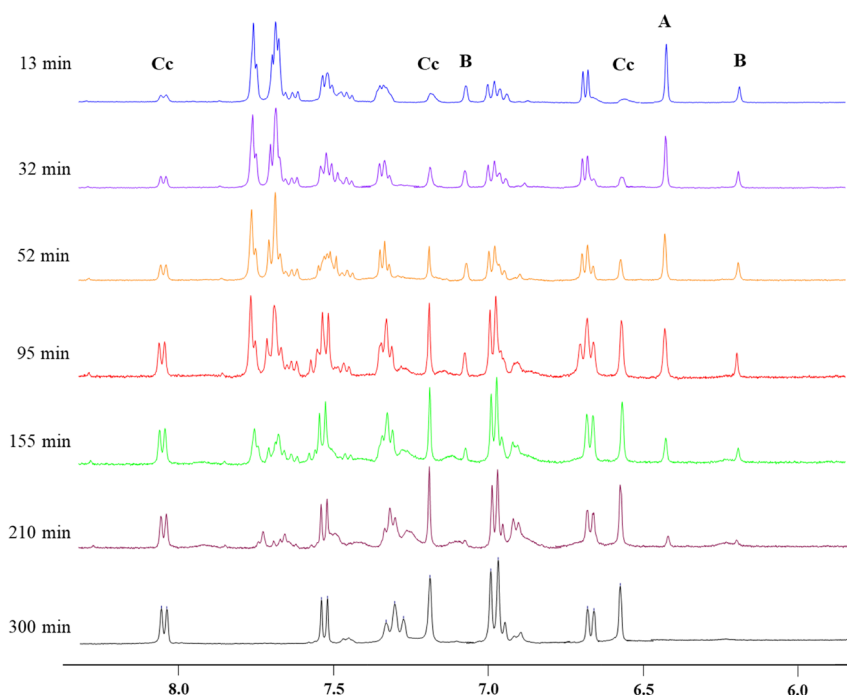
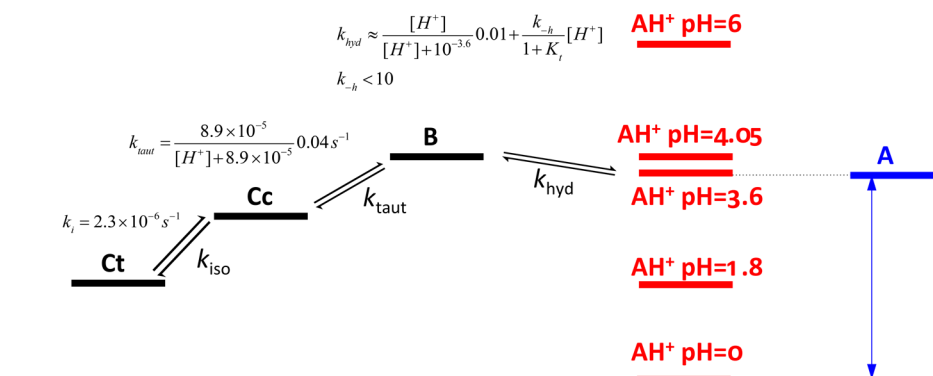


Figure 7. ^1H NMR spectra of compound **1** with the kinetics toward the pseudo-equilibrium in a DMSO/ D_2O (1:1) mixture at $\text{pD} = 5.8$ at different times.

The results can be summarized in [Scheme 3](#) and [Table 1](#).

Inspection of [Table 1](#) permits us to conclude that the 3,2'-*O*-bridge of the furan moiety of compound **1** stabilizes the quinoidal base and the hemiketal species in comparison with the model 4'-hydroxyflavylium cation.

Using the above values for the equilibrium and rate constants, the following energy level diagram for compound **1** in acidic medium can be drawn ([Scheme 4](#)).

NMR Experiments. The results above described were corroborated through a series of NMR experiments. Due to the limited solubility of compound **1** in water at neutral pH values, a DMSO/ D_2O mixture (1:1) was used to perform NMR experiments in this pH range. In this mixture of solvents, the absorption spectra behave similarly to water. In [Figure 6](#), the evolution of the multistate toward the pseudo-equilibrium after a direct pH jump to $\text{pD} = 5.8$ followed by ^1H NMR is shown.

Full characterization and assignment of ^1H and ^{13}C signals were achieved with correlation spectroscopy (COSY), heteronuclear single quantum coherence (HSQC) spectroscopy, and heteronuclear multiple bond coherence (HMBC) spectroscopy

([Table S2](#), [Supporting Information](#)) allowing the identification of the corresponding *cis*-chalcone structure, after 300 min of equilibration. The ^{13}C NMR signals at 182.7 and 149.4 ppm, assigned to carbons 5a and 10a, respectively (see [Table S2](#), [Supporting Information](#)), permit us to conclude that the furan ring is stable and does not undergo ring opening reaction under these conditions (see below).^{27,28}

The NMR data reported in [Figure 7](#) together with the results reported in [Figure 2a](#) show a large difference in the kinetics of compound **1** when compared with anthocyanins. The rates toward pseudo-equilibrium and equilibrium of compound **1** are remarkably slower than those of anthocyanins. However, the most significant difference is in the fact that hydration and tautomerization rates are similar, whereas in anthocyanins and related compounds, the tautomerization occurs in subseconds, and the hydration takes place in several minutes (except for very low pH values not accessed by direct pH jumps).

The remarkable difference of the kinetics between the present compound and anthocyanins and related compounds, which consists of the appearance and disappearance of B during the

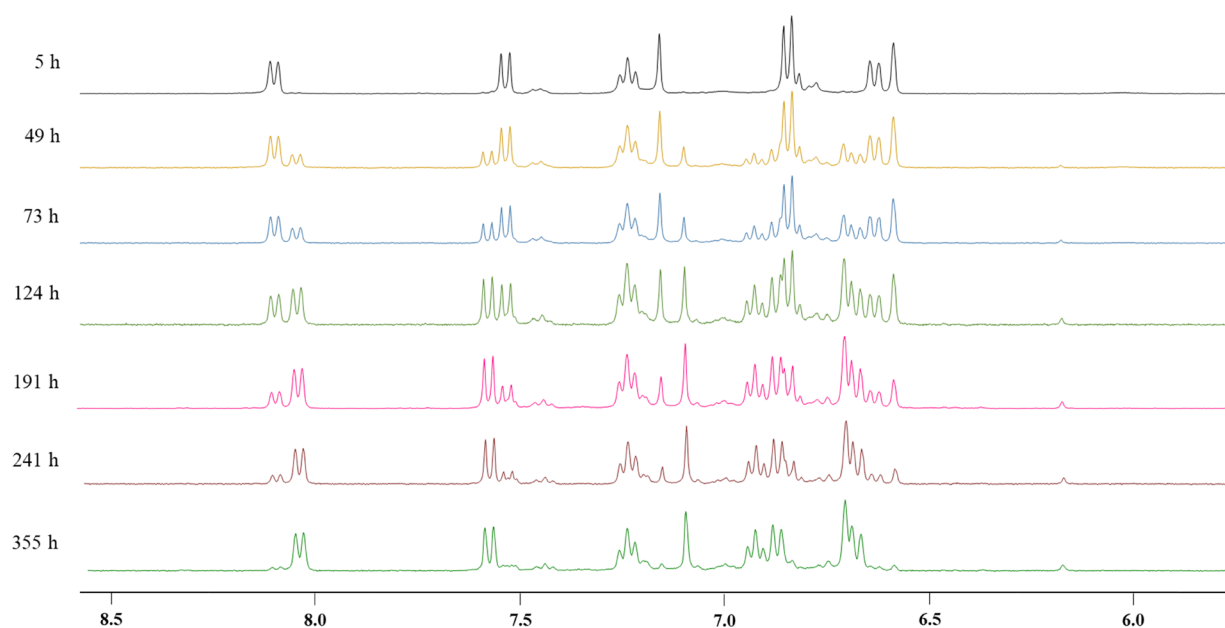


Figure 8. ^1H NMR of compound **1** in a $\text{DMSO-}d_6/\text{D}_2\text{O}$ (1:1) mixture at $\text{pD} = 6.3$ evolving from the pseudo-equilibrium toward the equilibrium.

first stages of the kinetics (Figure 2a) was confirmed by ^1H NMR (Figure 7). The rising and decreasing amount of B can only be explained if the difference between the rates of the hydration and tautomerization reactions is relatively small.

After reaching the pseudo-equilibrium, the system proceeds to the formation of *trans*-chalcone, a process that is almost completed only after 355 h (Figure 8). Full characterization and assignment of ^1H and ^{13}C signals were achieved with HSQC, HMBC, and COSY spectroscopy (Table S3, Supporting Information), allowing the identification of the *trans*-chalcone structure, after 355 h of equilibration. Similar to those of *cis*-chalcone, the ^{13}C NMR signals at 184.6 and 148.7 ppm, assigned to carbon atoms 5a and 10a, respectively (see Table S3, Supporting information), allow confirmation of the stability of the furan ring.^{27,28} The configuration of the double bond could be confirmed by comparing the chemical shift of C-11 in both chalcone-type structures. It has been reported that the resonance of C-11 of *trans*-aurones systematically occurs at approximately 10 ppm upfield from its position in *cis*-aurones;²⁸ in the aurones derived from compound **1**, the C-11 peaks at 117.0 ppm for *cis*-chalcone and at 108.7 ppm for *trans*-chalcone (Tables S2 and S3, Supporting Information).

To corroborate the stability of the furan ring in the structure, an aliquot of the equilibrated NMR tube solution (after 355 h) was analyzed by mass spectrometry. A base peak of m/z of 253 (negative ion mode) was detected. This result along with the NMR data obtained allows us to confirm the stability of the furan ring in the structure.

To characterize the species present under basic conditions, compound **1** was dissolved in H_2O , and the pH was adjusted up to 10.0 with 0.1 M aqueous NaOH solution. The evolution of the system was monitored by ^1H NMR, and it is similar to the one observed at $\text{pD} \approx 6$. The first spectrum collected approximately 15 min after the pH jump showed the presence of only one chalcone-type species. Full characterization and assignment of ^1H and ^{13}C signals were achieved with HSQC, HMBC, and COSY spectroscopy (Table S4, Supporting Information), allowing the identification of the corresponding doubly deprotonated *cis*-chalcone (Cc^{2-}). The ^{13}C NMR signals

at 180.3 and 148.9 ppm, assigned to carbon atoms 5a and 10a, respectively (see Table S4, Supporting information), allow us to propose that the furan ring is also stable under basic conditions.^{27,28} The system proceeds to full formation of the deprotonated *trans*-chalcone (Ct^{2-}) after 32 days. Full characterization and assignment of ^1H and ^{13}C signals for this species were achieved with HSQC, HMBC, and COSY spectroscopy (Table S5, Supporting Information). The ^{13}C NMR signals at 183.9 and 151.0 ppm, assigned to carbons 5a and 10a, respectively, prove the stability of the furan ring over this long period of equilibration.^{27,28} The configuration of the double bond has also been confirmed by comparing the chemical shift of C-11 in both chalcone-type structures:²⁸ C-11 peaks at 116.5 ppm for Cc^{2-} and at 108.2 ppm for Ct^{2-} (Tables S4 and S5, Supporting Information).

CONCLUSIONS

The synthetic furanoflavylum follows the same multistate of chemical species of simple flavylum cations and anthocyanins. Direct pH jumps of the flavylum cation from $\text{pH} = 1$ to higher pH values show that this species evolves slowly to the thermodynamically favorable *trans*-chalcone (*trans*-2'-hydroxyaurone) in two steps well separated with time: (i) from the flavylum cation and/or the quinoidal base to *cis*-chalcone via the hemiketal (which is observed as an intermediate species during the first stages of the kinetics) in a few hours, and ii) from *cis*-chalcone to *trans*-chalcones in a few weeks. On the other hand, the reverse pH jumps from higher pH values to $\text{pH} < 1$ reveal that *trans*-chalcone and *cis*-chalcone are metastable in accordance with the results previously reported for riccionidin A. In plant evolution, the species using aurones to give color have appeared before the species that use anthocyanins in the same scope. The interesting conclusion is that in both cases, the same basic multistate of chemical species is present. In other words, the anthocyanin multistate of chemical species has an ancestor in furanoflavylum derivatives.

EXPERIMENTAL SECTION

Materials and Methods. All solvents and chemicals employed for synthesis and preparation of samples were of reagent or spectrophotometric grade and used as received. Millipore-grade water was used. NMR spectra were run on a Bruker Advance III 400 spectrometer (400 MHz for ^1H , 100 MHz for ^{13}C) at 298 K. NMR assignments have been carried out on the basis of 1D NMR spectra (^1H , ^{13}C , and DEPT 135) and 2D NMR spectra (COSY, HSQC, and HMBC). Elemental analysis was performed on an elemental analysis system (Thermo Finnigan-CE Instruments Flash EA 1112 CHNS series). MS spectra were recorded in an Esquire 6000 spectrometer equipped with an ion trap analyzer (Esquire 6000; Bruker Daltonics). Data were acquired using an electrospray source in negative mode.

Thermodynamic and Kinetic Studies. The pH jumps were carried out by adding a stock solution of flavylum salt in 0.1 M HCl (1 mL) to a 3 mL quartz cuvette containing a solution of 0.1M NaOH (1 mL) and Theorell and Stenhagen universal buffer (1 mL)^{29f} at the desired final pH. This defined the ionic strength as 0.1 M (controlled by the NaCl concentration resulting from neutralization). The final pH of the solutions was measured using a Crison basic 20+ pH meter. Spectroscopic measurements were performed using Milli-Q water with a constant temperature of 20 ± 1 °C, with a Varian-Cary 100 Bio spectrophotometer.

Synthesis of 8-Hydroxybenzofuro[3,2-b]chromen-5-ium Hydrogen Sulfate (1). A mixture of 2-hydroxybenzaldehyde (0.122 mg; 1 mmol), 6-hydroxybenzofuran-3(2H)-one (0.150 g; 1 mmol), 98% H_2SO_4 (0.3 mL; 5.4 mmol), and HOAc (1.3 mL) was stirred for 6 h at room temperature following a similar procedure to that described previously by our group.³⁰ Then, Et_2O (50 mL) was added, and a red solid precipitated. The solid was filtered off, carefully washed with Et_2O , and dried, yielding the furanoflavylum salt **1** (0.282 g; 0.78 mmol; 80% yield). ^1H NMR (400 MHz, $\text{DMSO}-d_6$:TFA 4:1) δ 9.42 (s, 1H), 8.36 (m, 2H), 8.29 (d, $J = 7.7$ Hz, 1H), 8.14 (t, $J = 7.7$ Hz, 1H), 7.89 (t, $J = 7.7$ Hz, 1H), 7.31 (d, $J = 2.1$ Hz, 1H), 7.26 (dd, $J = 9.0, 2.1$ Hz, 1H). ^{13}C NMR (101 MHz, $\text{DMSO}-d_6$:TFA 4:1) δ 172.5, 168.0, 162.5, 153.2, 147.4, 136.3, 132.0, 130.1, 129.3, 127.7, 122.6, 120.0, 119.3, 107.7, 99.9. Elemental analysis (%): found C, 50.09; H, 3.42; S, 9.35; calcd. for $\text{C}_{15}\text{H}_{10}\text{SO}_7 \cdot 1.5 \text{H}_2\text{O}$: C, 49.86; H, 3.63; S, 8.87. A solution of compound **1** at pD of ~ 6.0 , equilibrated for 355 h, was analyzed by mass spectrometry. ITMS (ESI⁻): calcd. for $\text{C}_{15}\text{H}_9\text{O}_4$: m/z (%) 253.05 (100); found: 252.6 [M^-] (100).

NMR Experiments. NMR spectroscopy was performed by dissolving 5 mg of pure compound **1** in a mixture of $\text{DMSO}-d_6/\text{D}_2\text{O}$ (1:1) using 0.1 M NaOD to adjust the pD to ~ 6 . To avoid loss of proton signals under basic conditions due to exchange with deuterium, the compound was dissolved in H_2O , and the pH was adjusted to ~ 10 using 0.1 M NaOH. In this case, a closed tube containing D_2O was used inside the NMR tube for deuterium lock, and the water signal was suppressed by irradiation. Both NMR tubes were protected from light during the equilibration process. Some precipitation was observed at pH = 10.0, and after 32 days, it became necessary to heat the solution up to 60 °C for approximately 1 h. The 1D and 2D NMR experiments of equilibrated solution of compound **1** at pH = 10.0 were also performed at 60 °C.

ASSOCIATED CONTENT

Supporting Information

The Supporting Information is available free of charge on the ACS Publications website at DOI: 10.1021/acsomega.8b03696.

^1H , ^{13}C , and 2D NMR spectra and full peak assignment for several species present in the multistate system originating from compound **1** (PDF)

AUTHOR INFORMATION

Corresponding Authors

*E-mail: ajp@fct.unl.pt (A.J.P.).

*E-mail: fp@fct.unl.pt (F.P.).

ORCID

A. Alejo-Armijo: 0000-0001-8691-4628

A. Jorge Parola: 0000-0002-1333-9076

Fernando Pina: 0000-0001-8529-6848

Notes

The authors declare no competing financial interest.

ACKNOWLEDGMENTS

This work was supported by the Associate Laboratory for Green Chemistry- LAQV, which is financed by national funds from FCT/MCTES (UID/QUI/50006/2019). FCT/MCTES is also acknowledged through the National Portuguese NMR Network RECI/BBB-BQB/0230/2012. A.A.-A. is grateful for the postdoctoral fellowship from Fundación Alfonso Martí0n Escudero.

ADDITIONAL NOTES

^aIn acidic medium, these compounds give rise to styrylflavylum cations.

^bT. R. Seshadri has a large body of work on anthocyanin derivatives, coming from the school of Robert Robinson, his PhD supervisor.

^cWe noticed that during the XXIXth ICP, Madison, WI, USA, 2018, from the lecture by Professor Kevin Davies, he, in collaboration with Professor Øyvind Andersen has isolated and purified a natural aurone capable of giving the furanoflavylum cation, which is now under study by their groups.

^dSimilar shapes of the kinetic traces for AH^+/A , B, and Cc are observed if reversibility between B and Cc is considered.

^eKinetics of the ionized *trans*-chalcone is faster at basic pH values, and the titration was carried out from the ionized species back to their neutral form.

^fThe universal buffer used was prepared in the following way: 85% (w/w) phosphoric acid (2.3 mL), monohydrated citric acid (7.00 g), and boric acid (3.54 g) were dissolved in water; 1 M NaOH (343 mL) was then added, and the solution was diluted to 1 L with water.

REFERENCES

- (1) Furtado, P.; Figueiredo, P.; Chaves das Neves, H.; Pina, F. Photochemical and thermal degradation of anthocyanidins. *J. Photochem. Photobiol., A* **1993**, *75*, 113–118.
- (2) Cabrita, L.; Petrov, V.; Pina, F. On the thermal degradation of anthocyanidins: cyanidin. *RSC Adv.* **2014**, *4*, 18939–18944.
- (3) Sweeny, J. G.; Iacobucci, G. A. Effect of Substitution on the Stability of 3-Deoxyanthocyanidins in Aqueous Solutions. *J. Agric. Food Chem.* **1983**, *31*, 531–533.
- (4) Brouillard, R.; Iacobucci, G. A.; Sweeny, J. G. Chemistry of anthocyanin pigments. 9. UV-visible spectrophotometric determina-

tion of the acidity constants of apigeninidin and three related 3-deoxyflavylium salts. *J. Am. Chem. Soc.* **1982**, *104*, 7585–7590.

(5) Melo, M. J.; Moura, S.; Roque, A.; Maestri, M.; Pina, F. Photochemistry of luteolinidin: “Write-lock-read-unlock-erase” with a natural compound. *J. Photochem. Photobiol., A* **2000**, *135*, 33–39.

(6) Gomes, R.; Diniz, A. M.; Jesus, A.; Parola, A. J.; Pina, F. The synthesis and reaction network of 2-styryl-1-benzopyrylium salts: An unexploited class of potential colorants. *Dyes Pigm.* **2009**, *81*, 69–79.

(7) Gavara, R.; Petrov, V.; Pina, F. Characterization of the 4'-Hydroxynaphthoflavylium Network of Chemical Reactions. *Photochem. Photobiol. Sci.* **2010**, *9*, 298–303.

(8) Pina, F.; Melo, M. J.; Laia, C. A. T.; Parola, A. J.; Lima, J. C. Chemistry and Applications of Flavylium Compounds: a Handful of Colours. *Chem. Soc. Rev.* **2012**, *41*, 869–908.

(9) Petrov, V.; Diniz, A. M.; Cunha-Silva, L.; Parola, A. J.; Pina, F. Kinetic and thermodynamic study of 2'-hydroxy-8-methoxyflavylium. Reaction network interconverting flavylium cation and flavanone. *RSC Adv.* **2013**, *3*, 10786–10794.

(10) Moro, A. J.; Pana, A.-M.; Cseh, L.; Costisor, O.; Parola, J.; Cunha-Silva, L.; Puttreddy, R.; Rissanen, K.; Pina, F. Chemistry and Photochemistry of 2,6-bis(2-hydroxybenzylidene)cyclohexanone. An Example of a Compound Following the Anthocyanins Network of Chemical Reactions. *J. Phys. Chem. A* **2014**, *118*, 6208–6215.

(11) Alejo-Armijo, A.; Corici, L.; Cseh, L.; Aparaschivei, D.; Moro, A. J.; Parola, A. J.; Lima, J. C.; Pina, F. Achieving complexity at the bottom. 2,6-Bis(arylidene)cyclohexanones and Anthocyanins: the Same General Multistate of Species. *ACS Omega* **2018**, *3*, 17853–17862.

(12) Ono, E.; Fukuchi-Mizutani, M.; Nakamura, N.; Fukui, Y.; Yonekura-Sakakibara, K.; Yamaguchi, M.; Nakayama, T.; Tanaka, T.; Kusumi, T.; Tanaka, Y. Yellow flowers generated by expression of the aureone biosynthetic pathway. *Proc. Natl. Acad. Sci. U. S. A.* **2006**, *103*, 11075–11080.

(13) Kunz, S.; Burkhardt, G.; Becker, H. Riccionidins A And B, Anthocyanidins from the Cell Walls of the Liverwort *Ricciocarpos Natans*. *Phytochemistry* **1993**, *35*, 233–235.

(14) Chakravarty, G.; Seshadri, T. R. A study of 3, 2-furanoflavylium chlorides. *Indian J. Chem.* **1964**, *2*, 319–323.

(15) Davies, K. In Evolution of the flavonoid pathway for plant interaction with the abiotic and biotic environment, *XXIXth International Conference on Polyphenols (ICP)*, Madison, WI, 16-20 July 2018; University of Wisconsin: Madison, WI, 2018.

(16) Pina, F.; Melo, M. J.; Maestri, M.; Ballardini, R.; Balzani, V. Photochromism of 4'-Methoxyflavylium Perchlorate. A “Write-Lock-Read-Unlock-Erase” Molecular Switching System. *J. Am. Chem. Soc.* **1997**, *119*, 5556.

(17) Basilio, N.; Pina, F. Chemistry and Photochemistry of Anthocyanins and Related Compounds: A Thermodynamic and Kinetic Approach. *Molecules* **2016**, *21*, 1502.

(18) Pina, F. Thermodynamic and Kinetic Processes of Anthocyanins and Related Compounds and their Bio-Inspired Applications. In *Recent Advances in Polyphenols Research*; Romani, A.; Lattanzio, V.; Quideau, S., Eds.; Wiley-Blackwell: 2014, Chapter 11, vol. 4, 341-408.

(19) McClelland, R. A.; McGall, G. H. Hydration of the Flavylium Ion. 2. The 4'-Hydroxyflavylium Ion. *J. Org. Chem.* **1982**, *47*, 3730–3736.

(20) Pina, F.; Roque, A.; Melo, M. J.; Maestri, M.; Belladelli, L.; Balzani, V. Multistate/Multifunctional Molecular-Level Systems: Light and pH Switching between the Various Forms of a Synthetic Flavylium Salt. *Chem. - Eur. J.* **1998**, *4*, 1184–1191.

(21) Brouillard, R.; Delaporte, B.; Dubois, J. E. Chemistry of anthocyanin pigments. 3. Relaxation amplitudes in pH-jump experiments. *J. Am. Chem. Soc.* **1978**, *100*, 6202–6205.

(22) Pina, F. Chemical applications of anthocyanins and related compounds. A source of bioinspiration. *J. Agric. Food Chem.* **2014**, *62*, 6885–6897.

(23) Castet, F.; Champagne, B.; Pina, F.; Rodriguez, V. A Multistate pH-Triggered non-linear optical switch. *ChemPhysChem* **2014**, *15*, 2221–2224.

(24) Brouillard, R.; Dubois, J.-E. Mechanism of the structural transformations of anthocyanins in acidic media. *J. Am. Chem. Soc.* **1977**, *99*, 1359–1364.

(25) Moncada, M. C.; Parola, A. J.; Lodeiro, C.; Pina, F.; Maestri, M.; Balzani, V. Multistate/Multifunctional Behaviour of 4'-hydroxy-6-nitroflavylium: A Write-lock/Read/Unlock/Enable-erase/Erase Cycle Driven by Light and pH Stimulation. *Chem. - Eur. J.* **2004**, *10*, 1519–1526.

(26) Dyker, G.; Bauer, M. Synthesis of 2,3,6,8-Tetrahydroxybenzofuro[3,2-*b*][1]benzopyrylium Chloride (Riccionidin A). *Adv. Synth. Catal.* **1998**, *340*, 271–273.

(27) Löser, R.; Chlupacova, M.; Marecek, A.; Opletalova, V.; Gütschow, M. Synthetic Studies Towards the Preparation of 2-Benzyl-2-hydroxybenzofuran-3(2H)-one, the Prototype of Naturally Occurring Hydrated Auronols. *Helv. Chim. Acta* **2004**, *87*, 2597–2601.

(28) Agrawal, P. K.; Bansal, M. Other Flavonoids. In *Carbon-13 NMR of Flavonoids, Volume 39*; Agrawal, P. K., Ed.; Elsevier: Amsterdam, 1989, pp. 236-282.

(29) Küster, F. W.; Thiel, A.; Brückner, E. *Tabelle per Le Analisi Chimiche e Chimico-fisiche*. Hoepli: Milano, 1985, pp. 157–160.

(30) Calogero, G.; Sinopoli, A.; Citro, I.; Di Marco, G.; Petrov, V.; Diniz, A. M.; Parola, A. J.; Pina, F. Synthetic Analogues of Anthocyanins as Sensitizers for Dye-Sensitized Solar Cells. *Photochem. Photobiol. Sci.* **2013**, *12*, 883.